Cu(pc)I: A Molecular Metal with a One-Dimensional Array of Local Moments Embedded in a "Fermi Sea" of Charge Carriers

Michael Y. Ogawa,[†] Jens Martinsen,[†] Sharon M. Palmer,[†] Judith L. Stanton,[†] Jiro Tanaka,[§] Richard L. Greene,[‡] Brian M. Hoffman,*[†] and James A. Ibers*[†]

Contribution from the Department of Chemistry and Materials Research Center, Northwestern University, Evanston, Illinois 60201, IBM Research Laboratory, San Jose, California 95193, and the Department of Chemistry, Nagoya University, Chikusa, Nagoya, 464 Japan.
Received August 5, 1986

Abstract: Treatment of (phthalocyaninato)copper(II), Cu(pc), with elemental iodine affords (phthalocyaninato)copper iodide, Cu(pc)I. This material is comprised of metal-over-metal stacks of partially oxidized Cu(pc) groups surrounded by linear chains of I_3^- ions. Reflectivity spectra from single crystals of Cu(pc)I exhibit a very sharp plasma edge for light polarized parallel to the stacking direction and four-probe conductivity measurements show a room temperature conductivity of ca. $10^3\ \Omega^{-1}\ cm^{-1}$ along this direction. Together these measurements indicate that Cu(pc)I is the most highly conductive porphyrinic molecular metal studied to date and is among the most conductive molecular crystals known. Crystal data: tetragonal, space group D_{4h}^2-$P4/mcc$ with $a = 13.888$ (12) Å, $c = 6.390$ (8) Å, $V = 1232$ Å^3, and $Z = 2$. Thermoelectric power and magnetic susceptibility measurements show that the charge carriers of Cu(pc)I are holes in the $^5/_6$ filled band comprised of overlapping p-π orbitals from adjacent pc rings. The metal sites in this material retain their paramagnetic Cu^{2+} oxidation state, and thus Cu(pc)I represents the first example of a one-dimensional array of local moments embedded in a "Fermi sea" of charge carriers. The temperature dependence of the EPR g value for Cu(pc)I demonstrates a strong exchange coupling between the localized Cu^{2+} moments and the mobile charge carriers. An analysis of the temperature dependence of the EPR line width suggests that this exchange may include terms arising from dynamic and quantum mechanical exchange between local and mobile spins in addition to the dipolar and exchange interactions between neighboring Cu^{2+} sites that occur either directly or are mediated by the continuum of charge carrier states.

Highly conducting molecular crystals are usually divided into two categories: (1) organic molecular metals[1] that conduct through overlapping p-π molecular orbitals and (2) linear-chain metal-spine conductors[2] that propagate charge through metal-based d_{z^2} orbitals. We have shown that molecular metals based on metallomacrocycles[3-6] can represent either the first category, with charge transport through p-π orbitals of the macrocyclic ring,[4] *or* the second, with transport through the incorporated metal ions.[5] However, these materials also can show characteristics not possible in either of the two traditional classes of molecular conductors.[6] Earlier we showed that (tetrabenzoporphyrinato)-nickel(II) iodide, Ni(tbp)I, is a doubly mixed-valence conductor[6a] in which charge carriers propagate through a pathway that involves *both* metal and organic components. Here we report another novel situation that is possible only for conductors based on metal–organic compounds: (phthalocyaninato)copper iodide, Cu(pc)I, is the first molecular metal in which a linear array of metal-based local moments is embedded within a one-dimensional "Fermi sea" of organic charge carriers.

Cu(pc)I is a highly conducting ($\sigma_{RT} \approx 10^3\ \Omega^{-1}\ cm^{-1}$) molecular metal that belongs to the isostructural class of porphyrinic conductors characterized by metal-over-metal stacks of partially ($^1/_3$) oxidized M(pc) units surrounded by parallel chains of I_3^- ions. Thermoelectric power and magnetic susceptibility measurements show that Cu(pc)I is an exclusively ring-oxidized conductor and that its metal centers retain their intrinsically paramagnetic Cu^{2+} (d^9, $S = {}^1/_2$) oxidation state. Electron paramagnetic resonance (EPR) measurements provide clear evidence for a novel exchange coupling between the Cu^{2+} ions and π carriers within the conductive stacks of this unique molecular metal.

Interactions between localized spins and delocalized carriers also are seen in the well-studied case of magnetic impurities in three-dimensional atomic metals and are of interest because a simple one-electron picture cannot account for the existence of a localized moment if the impurity state is exchange-coupled to a continuum of carrier states.[7,8] Nonetheless, localized magnetic behavior has been observed in the presence of such interactions in cases where the impurity sites are magnetically dilute. Moreover, these intriguing atomic systems undergo a low-temperature transition to a state in which the impurity site has lost its local moment: the "Kondo transition".[8a] The situation presented here for Cu(pc)I is at once simpler and more complicated: Cu(pc)I presents a Kondo-type problem in one dimension;

[†] Northwestern University.
[‡] IBM Research Laboratory.
[§] Nagoya University.

(1) See, for example: (a) Proceedings of the International Conference on the Physics and Chemistry of Low Dimensional Synthetic Metals (ICSM 84) Parts C and D, Conducting Crystals, Pecile, C., Zerbi, G., Bozio, R., Girlando, A., Eds.; *Mol. Cryst. Liq. Cryst.* **1985**, *119* and **1985**, *120*. (b) Wudl, F. *Acc. Chem. Res.* **1984**, *17*, 227-232. (c) Williams, J. M.; Beno, M. A.; Wang, H. H.; Leung, P. C. W.; Emge, T. J.; Geiser, U.; Carlson, K. D. *Acc. Chem. Res.* **1985**, *18*, 261-267.

(2) See: Williams, J. M.; Schultz, A. J.; Underhill, A. E.; Carnerio, K. In *Extended Linear Chain Compounds*; Miller, J. S., Ed.; Plenum Press: New York, 1982; Vol. 1, pp 73-118.

(3) For a review, see (a) Hoffman, B. M.; Ibers, J. A. *Acc. Chem. Res.* **1983**, *16*, 15-21. (b) Palmer, S. M.; Stanton, J. L.; Martinsen, J.; Ogawa, M. Y.; Heuer, W. B.; Van Wallendael, S. E.; Hoffman, B. M.; Ibers, J. A. *Mol. Cryst. Liq. Cryst.* **1985**, *125*, 1-11. (c) Palmer, S. M.; Ogawa, M. Y.; Martinsen, J.; Stanton, J. L.; Hoffman, B. M.; Ibers, J. A.; Greene, R. L. *Mol. Cryst. Liq. Cryst.* **1985**, *120*, 427-432. (d) Euler, W. B.; Martinsen, J.; Pace, L. J.; Hoffman, B. M.; Ibers, J. A. *Mol. Cryst. Liq. Cryst.* **1982**, *81*, 231-242.

(4) (a) Schramm, C. J.; Stojakovic, D. R.; Hoffman, B. M.; Marks, T. J. *Science (Washington, DC)* **1978**, *200*, 47-48. (b) Schramm, C. J.; Scaringe, R. P.; Stojakovic, D. R.; Hoffman, B. M.; Ibers, J. A.; Marks, T. J. *J. Am. Chem. Soc.* **1980**, *102*, 6702-6713. (c) Martinsen, J.; Greene, R. L.; Palmer, S. M.; Hoffman, B. M. *J. Am. Chem. Soc.* **1983**, *105*, 677-678. (d) Martinsen, J.; Palmer, S. M.; Tanaka, J.; Greene, R. L.; Hoffman, B. M. *Phys. Rev. B* **1984**, *30*, 6269-6276. (e) Phillips, T. E.; Scaringe, R. P.; Hoffman, B. M.; Ibers, J. A. *J. Am. Chem. Soc.* **1980**, *102*, 3436-3443. (f) Pace, L. J.; Martinsen, J.; Ulman, A.; Hoffman, B. M.; Ibers, J. A. *J. Am. Chem. Soc.* **1983**, *105*, 2612-2620. (g) Palmer, S. M.; Stanton, J. L.; Hoffman, B. M.; Ibers, J. A. *Inorg. Chem.* **1986**, *25*, 2296-2300.

(5) Martinsen, J.; Stanton, J. L.; Greene, R. L.; Tanaka, J.; Hoffman, B. M.; Ibers, J. A. *J. Am. Chem. Soc.* **1985**, *107*, 6915-6920.

(6) (a) Martinsen, J.; Pace, L. J.; Phillips, T. E.; Hoffman, B. M.; Ibers, J. A. *J. Am. Chem. Soc.* **1982**, *104*, 83-91. (b) Ogawa, M. Y.; Hoffman, B. M.; Lee, S.; Yudowsky, M.; Halperin, W. P. *Phys. Rev. Lett.* **1986**, *57*, 1177-1180. (c) Ogawa, M. Y.; Palmer, S. M.; Martinsen, J.; Stanton, J. L.; Hoffman, B. M.; Ibers, J. A.; Lee, S.; Yudkowsky, M.; Halperin, W. P., *Synth. Met.* **1987**, *19*, 781-785.

(7) (a) Anderson, P. W. *Phys. Rev.* **1961**, *124*, 41-53. (b) Anderson, P. W. *Science (Washington, DC)* **1978**, *201*, 307-316.

(8) (a) Kondo, J. *Solid State Phys.* **1969**, *23*, 183-281. (b) Heeger, A. J. *Solid State Phys.* **1969**, *23*, 283-411.

0002-7863/87/1509-1115$01.50/0

Table I. Crystal Data and Experimental Details for Cu(pc)I

compd	Cu(pc)I
formula	$C_{32}H_{16}CuIN_8$
formula wt, g/mol	702.98
cell a, Å	13.888 (12)
c, Å	6.390 (8)
V, Å^3	1232
Z	2
density calcd, g/cm^3	1.894 (114 K)[a]
space group	D_{4h}^2–$P4/mcc$
crystal shape	needle of square cross sectn bounded by faces of the forms {100} and {001} with sepns of 0.059 and 0.551 mm, respctvly
crystal vol, mm^3	1.9×10^{-3}
radiation	graphite-monochromated Mo Kα (λ(Mo Kα_1) = 0.7093 Å)
μ, cm^{-1}	21.7[b]
take-off angle, deg	3.2
receiving aperture	5.7 mm wide by 4.0 mm high, 34 cm from the crystal
scan speed, °2θ/min	2
scan width	1.2° below Kα_1 to 1.1° above Kα_2
background counts	10s with rescan option[c] for $2\theta < 56°$, 20 s with rescan option for $56° \leq 2\theta \leq 60°$ [b]
data collected	$h \geq k \geq 0$, $l \geq 0$, $4 \leq 2\theta \leq 60°$
unique data	990
unique data with $F_o^2 > 3\sigma(F_o^2)$	513
no. of variables	65
R on F_o^2	0.084
R_w on F_o^2	0.131
R on F_o, $F_o^2 > 3\sigma(F_o^2)$	0.052
R_w on F_o, $F_o^2 > 3\sigma(F_o^2)$	0.057
error in obsd of unit wt	1.36 e^2

[a] The low-temperature system is based on a design by J. C. Huffman (Ph.D. Thesis, Indiana University, 1974). [b] Sample calculations of transmission factors revealed a range of 0.86–0.88, and so no correction was made for absorption effects. [c] The diffractometer was run under the disk-oriented Vanderbilt system (Lenhert, P. G. *J. Appl. Crystallogr.* **1975**, *8*, 568–570).

however, the local moments in this material are not isolated but exist in linear chains that exhibit dipolar and exchange interactions among Cu^{2+} sites as well as the coupling to the continuum of charge carrier states.

Experimental Section

Preparation of Cu(pc)I. Cu(pc) was purchased from Eastman Kodak Co. and was sublimed prior to use. Iodine was used as obtained from Mallinckrodt, Inc. Cu(pc)I was grown in H-tubes by reacting Cu(pc) with I_2 in a mixture of 1-chloronaphthalene and 1-methylnaphthalene at high temperatures ($T \sim 190$ °C). Crystals of Cu(pc)I exhibit the same green-bronze color and reflectivity as do crystals of Ni(pc)I.[4b] Visual inspection of material so prepared often discloses the presence of purple, unoxidized Cu(pc). Elemental analyses (Microtech Laboratories, Inc., Skokie, IL) on a number of samples from different batches are consistent with a Cu:I ratio of 1:1.00 ± 0.07. Anal. Calcd for $C_{32}H_{16}CuIN_8$: C, 54.52; N, 15.90. Found: C, 54.48; N, 15.98.

X-ray Diffraction Study of Cu(pc)I. On the basis of precession and Weissenberg X-ray photographs, crystals of Cu(pc)I were assigned to Laue group $4/mmm$ of the tetragonal system. The only systematic absences observed were for $0kl$ and hhl with l odd, consistent with space groups $P4/mcc$ or $P4cc$. Successful refinement of the structure supports the choice of the centrosymmetric space group D_{4h}^2–$P4/mcc$. The cell constants of $a = 13.888$ (12) and $c = 6.390$ (8) Å were determined at 114 K by least-squares refinement[9] of the setting angles of 15 automatically centered reflections on a Picker FACS-I diffractometer with the use of graphite-monochromated Mo Kα radiation. The intensities of the Bragg reflections were measured at 114 K by the θ–2θ scan technique and were processed with a value of p of 0.04 by methods standard in this laboratory.[10] No significant change was detected in the intensities of six standard reflections measured every 100 reflections. A total of 990 unique reflections was measured; of these 514 have $F_o^2 > 3\sigma(F_o^2)$. Experimental details and crystal data are given in Table I.

Precession and Weissenberg photographs of Cu(pc)I are indistinguishable from those of Ni(pc)I. Hence the atomic coordinates of Ni(pc)I[4b] were used as the starting coordinates in the full-matrix, least-squares refinement of the data for Cu(pc)I. After a cycle of refinement in which the non-hydrogen atoms were allowed to vibrate anisotropically, the positions of the four independent hydrogen atoms were added as fixed contributions to the structure factors in ensuing cycles. It was assumed that each H atom could be idealized with a C–H bond length of 0.95 Å and an isotropic thermal parameter 1 Å^2 greater than the equivalent isotropic thermal parameter of the C atom to which it is bonded. The final cycle of refinement was carried out on F_o^2 and involved 65 variables and 990 observations (including those for which $F_o^2 < 0$). This refinement converged to the agreement indices given in Table I. An analysis of $\sum w(F_o^2 - F_c^2)^2$ as a function of setting angles, F_o^2, and Miller indices reveals no unexpected trends. The maximum and minimum electron densities on a final difference electron density synthesis are 2.7 and −3.0 e/Å^3. The height of a C atom in this structure is about 12 e/Å^3.

Final positional and isotropic thermal parameters are given in Table II. Table III displays the anisotropic thermal parameter while Table IV provides a listing of $10|F_o|$ vs. $10|F_c|$.[11]

Resonance Raman Spectra. Raman spectra were obtained at ambient temperatures from crystalline and microcrystalline samples contained in 5-mm Pyrex tubes. The tubes were spun (~1200 rpm) to eliminate decomposition of the sample by the laser. The spectra were recorded on a spectrometer described elsewhere[12] with the use of a 5145 Å Ar^+ laser line as the excitation source and were corrected, where necessary, for the plasma line.

Single-Crystal Polarized Reflectivity Spectra. Room temperature single-crystal polarized reflection spectra were measured for Cu(pc)I both along the highly conducting stacking axis and perpendicular to it. The measurements were made with a microspectrophotometer consisting of a Carl–Zeiss double monochromator, tungsten source, a microscope with reflecting and quartz lenses, and a detector system utilizing a photomultiplier tube (Hammatsu Photonics Co. Ltd, R928) and PbS or InSb IR detectors (Santa Barbara Research Center). The monochromatic light was polarized with a MgF_2 polarizer. Absolute reflectivities were calibrated with a SiC standard. The reflectance spectra were measured between 3 and 25 kK.

Charge Transport Measurements. Single crystals of Cu(pc)I were mounted on silvered graphite fibers, and four-probe ac conductivity measurements were performed along the stacking axis at temperatures between 400 and 20 K, as described previously.[13] Thermoelectric power (TEP) measurements along the same axis at temperatures between 300 and 10 K were obtained on an apparatus also described earlier.[14] Temperature variability was accomplished by placing the copper thermal block in an Air Products LTR-3 Helitran. A slow sinusoidal thermal cycling technique was employed that generates a maximum temperature gradient of 0.5 K across the sample.

Magnetic Susceptibility Measurements. Static magnetic susceptibility measurements were taken from 300 to 1.7 K with a SHE VTS-50 SQUID susceptometer. Sample holders made of high purity Spectrosil quartz (Thermal American Inc., NJ) were employed. The background was obtained over the full temperature range just prior to measuring the sample and was also checked at several temperatures afterwards. Calibration of the instrument was routinely checked with $HgCo(SCN)_4$ as a standard. Although field dependence studies revealed no significant deviations up to 50 kG at various temperatures, the measurements were routinely performed at either 5 or 15 kG. Sample sizes varied from 15 to 50 mg, with 40 mg being the average size.

Electron Paramagnetic Resonance Measurements. Variable temperature EPR spectra at X-band frequencies (ca. 9 GHz) were obtained down to 100 K as described elsewhere.[4b] Temperatures down to 4.2 K were obtained with an Air Products Model LTR cryostat system in combination with a Scientific Instruments Series 5500 microprocessor-based temperature controller. The sample temperature, stable to within ±0.5 K at 100 K and to within ±0.2 K at base temperature, was monitored with a calibrated silicon diode cryogenic temperature sensor (Lakeshore Cryotronics, DT-5000 DRC) placed to within 5 mm of the sample.

Results

Resonance Raman Spectroscopy. The resonance Raman spectrum of polycrystalline Cu(pc)I at room temperature exhibits

(9) Corfield, P. W. R.; Doedens, R. J.; Ibers, J. A. *Inorg. Chem.* **1967**, *6*, 197–204.
(10) See, for example: Waters, J. M.; Ibers, J. A. *Inorg. Chem.* **1977**, *16*, 3273–3277.
(11) Supplementary Material.
(12) Shriver, D. F.; Dunn, J. B. R. *Appl. Spectrosc.* **1974**, *28*, 319–323.
(13) Phillips, T. E.; Anderson, J. R.; Schramm, C. J.; Hoffman, B. M. *Rev. Sci. Instrum.* **1979**, *50*, 263–265.
(14) Chaikin, P. M.; Kwak, J. F. *Rev. Sci. Instrum.* **1975**, *46*, 218–220.

Table II. Positional Parameters and B_{eq} for Cu(pc)I

atom	x	y	z	B (Å^2)	atom	x	y	z	B (Å^2)
I	1/2	1/2	1/4	2.94 (3)	C(5)	0.44631 (52)	0.15309 (57)	0	1.8 (2)
Cu	0	0	0	1.10 (3)	C(6)	0.39053 (56)	0.07016 (57)	0	1.7 (2)
N(1)	0.12587 (38)	0.05980 (40)	0	0.9 (1)	C(7)	0.29088 (51)	0.08158 (49)	0	1.2 (2)
N(2)	0.08280 (42)	0.22815 (42)	0	1.3 (1)	C(8)	0.21253 (46)	0.01132 (60)	0	1.4 (2)
C(1)	0.14509 (56)	0.15638 (55)	0	1.2 (2)	HlC(3)	0.277	0.318	0	2.8
C(2)	0.24910 (51)	0.17232 (46)	0	1.3 (2)	HlC(4)	0.444	0.300	0	3.3
C(3)	0.30441 (54)	0.25584 (53)	0	1.7 (2)	HlC(5)	0.514	0.148	0	2.9
C(4)	0.40424 (58)	0.24510 (61)	0	2.1 (2)	HlC(6)	0.419	0.009	0	2.8

Table V. Bond Distances and Angles for Cu(pc)I

Distances, Å

Cu-N(1)	1.935 (6)	C(2)-C(7)	1.388 (10)
N(1)-C(1)	1.367 (9)	C(3)-C(4)	1.395 (10)
N(1)-C(8)	1.370 (9)	C(4)-C(5)	1.405 (11)
N(2)-C(1)	1.320 (10)	C(5)-C(6)	1.388 (11)
N(2)-C(8)	1.325 (10)	C(6)-C(7)	1.393 (10)
C(1)-C(2)	1.461 (10)	C(7)-C(8)	1.462 (9)
C(2)-C(3)	1.391 (10)		

Angles, deg

N(1)-Cu-N(1)	90.00	C(2)-C(3)-C(4)	117.4 (7)
Cu-N(1)-C(1)	126.7 (5)	C(3)-C(4)-C(5)	120.7 (7)
Cu-N(1)-C(8)	125.4 (5)	C(4)-C(5)-C(6)	121.5 (7)
C(1)-N(1)-C(8)	108.0 (6)	C(5)-C(6)-C(7)	117.4 (7)
C(1)-N(2)-C(8)	121.5 (6)	C(2)-C(7)-C(6)	121.3 (7)
N(1)-C(1)-N(2)	127.8 (7)	C(2)-C(7)-C(8)	107.2 (6)
N(1)-C(1)-C(2)	110.0 (7)	C(6)-C(7)-C(8)	131.6 (7)
N(2)-C(1)-C(2)	122.2 (6)	N(1)-C(8)-N(2)	128.6 (6)
C(1)-C(2)-C(3)	132.2 (6)	N(1)-C(8)-C(7)	108.9 (7)
C(1)-C(2)-C(7)	106.0 (6)	N(2)-C(8)-C(7)	122.5 (6)
C(3)-C(2)-C(7)	121.8 (6)		

a sharp fundamental peak at 107 cm^{-1} with an overtone progression of peaks at 213, 320, and 436 cm^{-1}. This pattern is characteristic of linear chains of symmetrical triiodide ions.[15] The absence of any observable peaks having an intensity larger than that of the overtone band at either 167 or 212 cm^{-1} eliminates I_5^- or I_2 as being the predominant iodine form in this material. By analogy with Ni(pc)I,[4b] for which ^{129}I Mössbauer experiments provided no evidence for the presence of I^-, we conclude that Cu(pc)I also contains no I^- ions. Thus, the proper formulation of Cu(pc)I is $[Cu(pc)]_2[Cu(pc)^+][I_3^-]$ or in the mixed valence notation $[Cu(pc)]^{+0.33}[I_3^-]_{0.33}$ to indicate partial oxidation of 1/3 electrons per metallomacrocycle.

Description of the Structure. As expected from similarities in unit cell constants and X-ray photographs, the structure of Cu(pc)I is essentially the same as that of Ni(pc)I.[4b] It consists of columns of Cu(pc) molecules segregated from chains of I_3^- anions. Each ring is on a site of $4/m$ symmetry and is thus constrained to be planar. The rings stack metal-over-metal with the plane of the rings normal to the stacking axis. Successive rings in the unit cell are staggered by 39.2 (3)°. Each I atom lies on a site of 422 symmetry. Chains of I_3^- anions lie in the channels between Cu(pc) stacks. Each iodine chain is ordered along the length of the chain but disordered with respect to other I_3^- chains. This disorder gives rise to the abnormally high value of U_{33} for I and to diffuse X-ray scattering in planes perpendicular to the stacking axis. The nature of this disorder has been discussed in detail for Ni(pc)I.[4b]

Bond distances and angles for Cu(pc)I are listed in Table V. All bond distances in Cu(pc)I agree with those in Ni(pc)I within experimental error except for the M-N(1) distance, which is 1.887 (6) Å in Ni(pc)I and 1.935 (6) Å in Cu(pc)I. As a result of this change in M-N(1) distance, there are some changes in bond angles between these two compounds.

Single-Crystal Polarized Reflectivity Measurements. The polarized room temperature reflectance spectra of Cu(pc)I are shown in Figure 1. With the electric field vector oriented perpendicular to the highly conducting stacking (c axis) direction, peaks are found at 25, 17.3, and 14.8 kK; these are assigned to the in-plane $\pi_g^* \leftarrow \pi_u$ transitions of the phthalocyanine ring.[16] The positions of these bands are in accord with those of Ni(pc)I. At low frequency the reflectivity is small and exhibits no features attributable to intraband transitions. In the spectrum measured with light polarized parallel to the stacking axis, a strong peak found at 18.5 kK can be assigned to the $\sigma_u^* \leftarrow \sigma_g$ transition of the I_3^- chain.[17] More importantly the reflectivity rises steeply in the near-infrared region at 4 kK, behavior that is characteristic of quasi one-dimensional metallic conductivity in Cu(pc)I crystals. The shape of the plasma edge is qualitatively similar to that for Ni(pc)I, but the band edge is much sharper. The following calculation indicates a more metallic character for Cu(pc)I.

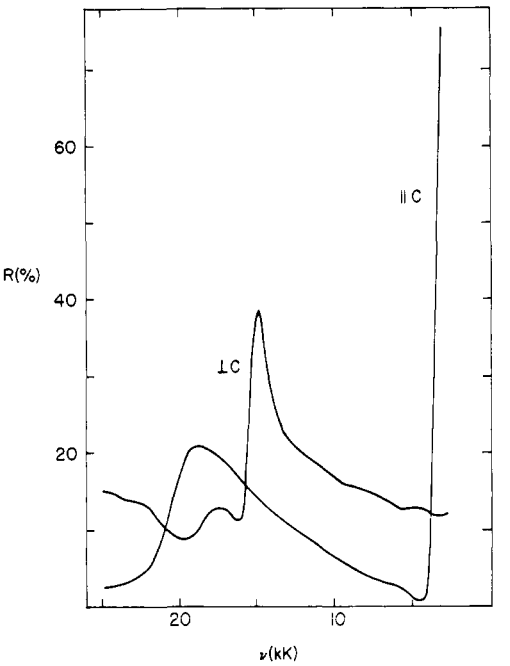

Figure 1. Room temperature polarized reflectance spectrum of a single crystal of Cu(pc)I. The perpendicular (⊥) orientation has the electric field polarized normal to the highly conducting needle axis while the parallel (∥) orientation has the electric field polarized along this axis.

The dielectric response function $\epsilon(\omega)$ of a metal is given by the Drude model as[18]

$$\epsilon(\omega) = \epsilon_{core} - \frac{\omega_p^2}{\omega_2 - i\omega/\tau} = \epsilon_1 + i\epsilon_2 \quad (1)$$

where

$$\omega_p^2 = \frac{4\pi Ne^2}{m^*} \quad (2)$$

ϵ_{core} is the residual dielectric constant at high frequency arising

(15) (a) Teitelbaum, R. C.; Ruby, S. L.; Marks, T. J. *J. Am. Chem. Soc.* **1978**, *100*, 3215-3217. (b) Teitelbaum, R. C.; Ruby, S. L.; Marks, T. J. *J. Am. Chem. Soc.* **1980**, *102*, 3322-3328.

(16) Lever, A. B. P. *Adv. Inorg. Chem. Radiochem.* **1965**, *7*, 28-105.
(17) Mizuno, M.; Tanaka, J.; Harada, I. *J. Phys. Chem.* **1981**, *85*, 1789-1794.
(18) Ashcroft, N. W.; Mermin, N. D. *Solid State Physics*; Saunders College: Philadelphia, 1976.

from core polarizability, τ is the electronic relaxation time, ω_p is the plasma frequency, and N is the number of carriers per unit volume. Thermoelectric power measurements (vide infra) clearly indicate that the charge carriers of Cu(pc)I are holes in the $^5/_6$ filled π band derived from the highest occupied orbital of the pc ring. The number of charge carriers per site generated by partial oxidation is $\rho = {}^1/_3$ and with two Cu(pc) units per unit cell, $N = 2(2-\rho)/|\hat{a} \times \hat{b} \times \hat{c}|$. The reflectance is given in terms of the real and imaginary parts of ϵ by[19]

$$R = \frac{1 + |\epsilon| - [2(|\epsilon| + \epsilon_1)]^{1/2}}{1 + |\epsilon| + [2(|\epsilon| + \epsilon_1)]^{1/2}} \quad (3)$$

where

$$|\epsilon| = (\epsilon_1^2 + \epsilon_2^2)^{1/2}$$

Upon fitting the parallel polarized data below 4 kK in Figure 1 to eq 3 we find the parameters $\omega_p = 6670$ cm^{-1}, $\tau = 1.36\ (3) \times 10^{-14}$ s, and $\epsilon_{core} = 3.4\ (2)$.

Band structure and transport parameters may be calculated from the reflectance parameters. The effective carrier mass is obtained from eq 2 with $N = 2.6 \times 10^{21}$ cm^{-3}, as calculated from the X-ray data; we obtain $m^* = 5.3$ m_e, where m_e is the free-electron mass. The one-dimensional tight-binding bandwidth ($4t$) is evaluated from the formula[20]

$$t = \frac{(\hbar\omega_p)^2}{16Ne^2d^2 \sin\frac{\pi\rho}{2}} \quad (4)$$

where $d = 3.195\ (4)$ Å is the interphthalocyanine spacing along the stacking axis. We obtain $4t = 1.45$ eV. The optical dc conductivity σ_{opt} can also be obtained from the parameters of eq 3 by

$$\sigma_{opt} = \frac{\omega_p^2}{4\pi}\tau \quad (5)$$

The calculated value of $\sigma_{opt} = 1900\ \Omega^{-1}$ cm^{-1} is in agreement with that of ca. 2000 Ω^{-1} cm^{-1} obtained from four-probe conductivity measurements (vide infra). Presumably, the same scattering process dominates the optical and the dc conductivities.

This suggestion is supported by a comparison of the electron–phonon interaction at dc and optical frequencies. Hopfield[21] has presented an expression for the total phonon scattering rate at optical frequencies

$$\tau^{-1} = \lambda_1(2\pi k_B/\hbar)(T + T_\theta) \quad (6)$$

where λ_1 is a dimensionless electron–phonon coupling constant and T_θ is the Debye temperature. For $T >> T_\theta$, as is usual at room temperature, eq 6 may be rearranged to yield

$$\lambda_1 = \hbar/(2\pi\tau k_B T) \quad (7)$$

For Cu(pc)I at room temperature we obtain $\lambda_1 = 0.3$, somewhat less than for Ni(pc)I[4d] ($\lambda_1 = 0.6$) and TTF·TCNQ[22] ($\lambda_1 = 1.3$). The value for Cu(pc)I is comparable with those for good metals such as copper[18] ($\tau = 2.7 \times 10^{-14}$ s and $\lambda_1 = 0.1$) and sodium[18] ($\tau = 3.2 \times 10^{-14}$ s and $\lambda_1 = 0.11$).

An alternative expression for the electron–phonon coupling, which includes lifetime terms, involves the temperature variation of the dc resisitivity ρ,

$$\lambda_2 = \frac{\hbar\omega_p^2}{2\pi k_B}\frac{\partial\rho}{\partial T} \quad (8)$$

The parameter λ_2 can be evaluated from a value of 2.0×10^{-6} Ω cm/K for $\partial\rho/\partial T$ calculated from the fit of the resistivity; the result is $\lambda_2 = 0.33$. The close agreement between λ_1 and λ_2 clearly indicates that at room temperature carrier scattering in Cu(pc)I is dominated by phonon contributions.

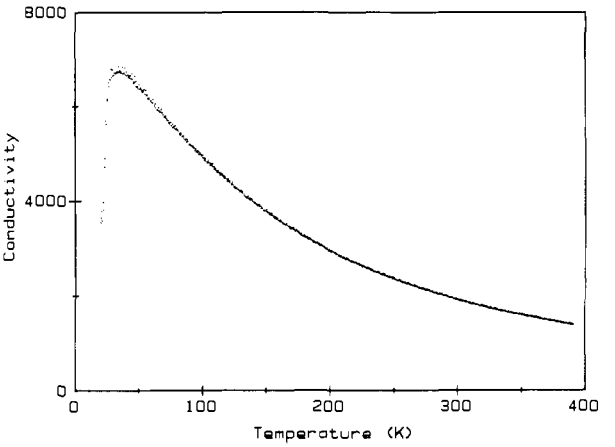

Figure 2. Four-probe single-crystal conductivity (Ω^{-1} cm^{-1}) of Cu(pc)I taken along the stacking axis as a function of temperature. The conductivity maximum at ca. 50 K is believed to be an extrinsic phenomena, as described in the text.

Charge Transport Measurements. Single crystals of Cu(pc)I exhibit a conductivity in the range of ca. 10^3 Ω^{-1} cm^{-1} along the stacking direction at room temperature. There is a metallic rise in conductivity ($d\sigma/dT < 0$) throughout the temperature range 390–50 K (Figure 2) for which the resistivity may be fit to the expression for a metal

$$\rho(T) = \rho_0 + \rho_1 T^\gamma \quad (9)$$

where $\rho_0 = 1.33 \times 10^{-4}$ Ω cm, $\rho_1 = 5.44 \times 10^{-8}$ Ω cm K$^{-\gamma}$, and $\gamma = 1.56$. The exponent, γ, is consistent with that obtained for the homologous compound, Ni(pc)I[4d] ($\gamma = 1.65$–1.75), where the dependence of ρ on T has been explained as the consequence of carrier scattering by a combination of one-phonon and two-libron processes.[23]

The conductivity of all crystals of Cu(pc)I measured to date reaches a maximum value at temperatures of 20 K or above and decreases upon further cooling. However, both the magnitude of these conductivity maxima and the temperatures at which they occur are extremely crystal dependent. We believe that this phenomenon primarily reflects a degree of thermal stress on the crystal mounts and is not an intrinsic property of this material. This conclusion is supported by the thermoelectric power measurements now discussed.

Thermoelectric Power Measurements. Thermoelectric power measurements[24] provide the sign of the predominant charge carriers in a conductive material. For Cu(pc), oxidation from the filled π orbitals of the pc ring would create a conduction band for the Cu(pc) stack that is $^5/_6$ filled; conduction would be by holes and the Seebeck coefficient (S) would be positive. In contrast, oxidation of $^1/_3$ electron per site from the half-filled Cu^{2+} $d_{x^2-y^2}$ orbitals would give rise to a conduction band for the stack that is only $^1/_3$ filled; conduction would be by electrons and S would be negative.

The temperature response of S for a typical sample of Cu(pc)I is shown in Figure 3; the thermoelectric power is positive throughout the temperature range, $10\ K \leq T \leq 300$ K. Thus the principal charge carriers are holes. Hence, the site of oxidation must be the ligand π-system, as for Ni(pc)I,[4a-d] and not the metal center, as for Co(pc)I.[5] The conclusion that oxidation in Cu(pc)I occurs from ligand-based orbitals is consistent with the high electrical conductivity of this material; it would be unreasonable to associate such high conductivity with a conduction band produced by δ bonding between in-plane copper $d_{x^2-y^2}$ orbitals that are 3.2 Å apart.

The thermoelectric power of highly conducting materials also serves to determine their band parameters and is extremely sen-

(19) Wooten, F. *Optical Properties of Solids*; Academic: New York, 1972.
(20) Torrance, J. B.; Scott, B. A.; Welber, B.; Kaufman, F. B.; Seiden, P. E. *Phys. Rev. B.* **1979**, *19*, 730–741.
(21) Hopfield, J. J. *Comments Solid State Phys.* **1970**, *3*, 48–52.
(22) Bright, A. A.; Garito, A. F.; Heeger, A. J. *Phys. Rev. B* **1974**, *10*, 1328–1342.
(23) Hale, P. D.; Ratner, M. A. *J. Chem. Phys.* **1985**, *83*, 5277–5285.
(24) Fritzsche, H. *Solid State Commun.* **1971**, *9*, 1813–1815.

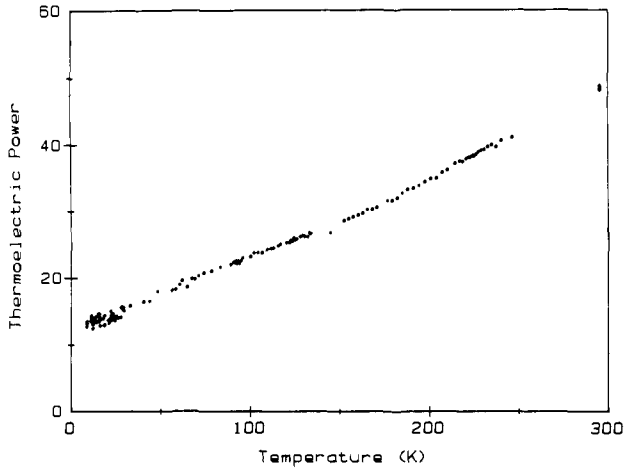

Figure 3. Temperature dependence of the thermoelectric power (Seebeck coefficient, $\mu V/K$) of a single crystal of Cu(pc)I taken along the needle axis.

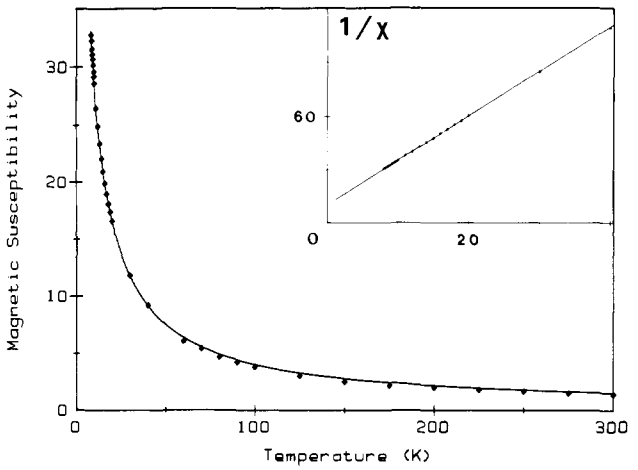

Figure 4. Bulk paramagnetic susceptibility (χ) of Cu(pc)I as a function of temperature. Inset: plot of χ^{-1} vs. temperature within the range of $8 \leq T \leq 40$ K. The solid line in both the figure and the inset represents the best fit to eq 11 as described in the text.

sitive to alterations of the density of states at the Fermi level that would result from a metal to nonmetal phase transition. The tight-binding band model predicts that the thermoelectric power of a one-dimensional metal will vary linearly with temperature[25]

$$S = -[\pi^2 k_B^2 \cos(\pi\nu/2)/6|e|\, t \sin^2(\pi\nu/2)]T \quad (10)$$

where t is the transfer integral ($4t$ = bandwidth), k_B is Boltzmann's constant, e is the electron charge, and $\nu = (2-\rho)$ is the number of conduction band electrons per site when ρ is the degree of oxidation. As seen in Figure 3, the thermoelectric power of Cu(pc)I does in fact vary linearly with temperature over the range studied. This linear dependence indicates that no major change in the density of states at the Fermi level occurs for Cu(pc)I within the temperature range $10 < T \leq 300$ K and that the observed maxima in the conductivity data above 10 K are indeed extrinsic. However, the thermoelectric power data do not exhibit the zero intercept expected for a metal; rather the intercept is around 10–15 $\mu V/K$. Although this result is not understood, a nonzero intercept has been observed in other molecular conductors that contain I_3^- units,[26] Ni(pc)I being an exception.[4d] Upon equating the temperature coefficient of eq 10 with the slope of a linear least-squares fit to the thermoelectric power data, we obtain $t = 0.31$ (1) eV and a bandwidth of 1.24 eV, larger than the 0.88 eV for Ni(pc)I[4d] and in good agreement with that obtained from the polarized reflectance measurements (1.45 eV).

Magnetic Susceptibility Measurements. At 300 K, the static paramagnetic susceptibility of Cu(pc)I is 1.38×10^{-3} emu mol^{-1} when corrected for the diamagnetism of triiodide, the pc ring, and the metal center. This value corresponds to approximately 1.1 unpaired electron spins ($S = {}^1/_2$, $g \sim 2$) per metallomacrocycle and provides additional support for the conclusion that oxidation does not occur at the Cu^{2+} metal sites in this material. Oxidation of ${}^1/_3$ of the paramagnetic metal centers in Cu(pc) could lead to a paramagnetic susceptibility of no more than ${}^2/_3$ spins per macrocycle. However, partial oxidation of the pc ring would leave the Cu^{2+} centers intact and would create π-charge carriers that exhibit a Pauli paramagnetism, thereby giving rise to a total susceptibility of greater than one spin per formula unit.

The temperature dependence of the paramagnetic susceptibility of Cu(pc)I over the temperature range $10 \leq T \leq 300$ K is shown in Figure 4. Within this range the susceptibility increases upon cooling and obeys the relation

$$\chi^{(T)} = \chi_{Cu}{}^{(T)} + \chi_\pi = \frac{C}{T-\theta} + \chi_\pi \quad (11)$$

This expression includes a temperature-dependent contribution from localized Cu^{2+} spins, $\chi_{Cu}{}^{(T)}$, expressed in a Curie–Weiss form, and a temperature independent Pauli susceptibility associated with the organic charge carriers, χ_π. To characterize best the local-spin parameters, we have analyzed the low-temperature data, $8 \leq T \leq 40$ K, according to eq 11. However, in that regime χ_π contributes negligibly and thus is not determined accurately. Therefore, we employed a value, $\chi_\pi = 3.8 \times 10^{-5}$ emu mol^{-1}, that is obtained from χ_π for Ni(pc)I by scaling with the bandwidths determined from the reflectance spectra: χ_π(Cu(pc)I) = χ_π(Ni(pc)I) × (t(Ni(pc)I)/t(Cu(pc)I)). The result is $C = 0.401$ (2) emu K mol^{-1} and $\theta = -4.18$ (3) K. Figure 4 shows good agreement between the experimental and theoretical values of $\chi^{-1(T)}$ over the whole range of temperatures. The value of C obtained from this fit is in excellent agreement with $C = 0.402$ emu K mol^{-1} calculated for one copper spin per site

$$C = S(S+1)(Ng^2\mu_B{}^2/3k_B)$$

where N is Avogadro's number, μ_B is the Bohr magneton, k is Boltzmann's constant, S is the electron spin, and g^2 is the average Cu g^2 value. This result confirms a picture of Cu(pc)I in which each Cu site is fully occupied by a Curie-like local moment that coexists with the π-spin charge carriers.

The Weiss constant may have two separate contributions. A nonconducting one-dimensional Heisenberg chain of copper spins would have a Weiss constant, $\theta_{dir} = J_{dd}/k_B$ where J_{dd} is the strength of the near-neighbor Cu–Cu exchange parameter.[27] In addition, by analogy to the case of isolated magnetic impurities in a three-dimensional metal,[28] exchange between local moments and itinerant carriers of strength $J_{d\pi}$ would give a contribution to the Weiss constant for the local moments, $\theta_{ind} \propto [J_{d\pi}]^2\rho$, where ρ is the density of states at the Fermi level. As a first approximation for the novel situation presented by Cu(pc)I, we propose that $\theta_{obsd} = \theta_{dir} + \theta_{ind}$. ^{1}H NMR measurements discussed elsewhere[6b,c] suggest that the value of θ_{dir} for Cu(pc)I is small and that the exchange energy involving Cu^{2+} sites is dominated by coupling through the itinerant carrier spins. This possibility is supported by the work of Reed and co-workers,[29] who observed d–π coupling in π-cation radicals of copper and iron porphyrins.

EPR g Values. The preceding discussion shows that Cu(pc)I exhibits an array of localized Cu^{2+} spins (one per site) as well as a system of mobile charge carriers. In the absence of exchange interactions between these two spins systems, the EPR spectrum

(25) Chaikin, P. M.; Kwak, J. F.; Jones, T. E.; Garito, A. F.; Heeger, A. J. *Phys. Rev. Lett.* **1973**, *31*, 601–604.
(26) (a) Khanna, S. K.; Yen, S. P. S.; Somoano, R. B.; Chaikin, P. M.; Ma, C. L.; Williams, R.; Samson, S. *Phys. Rev. B* **1979**, *19*, 655–663. (b) Somoano, R. B.; Yen, S. P. S.; Hadek, V.; Khanna, S. K.; Novotny, M.; Datta, T.; Hermann, A. M.; Woodlam, J. A. *Phys. Rev. B* **1977**, *17*, 2853–2857.
(27) Smart, J. S. *Effective Field Theories of Magnetism*; W. B. Saunders: Philadelphia, 1966.
(28) Barnes, S. E. *Adv. Phys.* **1981**, *30*, 801–938.
(29) (a) Gans, P.; Buisson, G.; Duee, E.; Marchon, J.-C.; Erler, B. S.; Scholz, W. F.; Reed, C. A. *J. Am. Chem. Soc.* **1986**, *108*, 1223–1234. (b) Scholz, W. F.; Reed, C. A.; Lee, Y. J.; Scheidt, W. R.; Lang, G. *J. Am. Chem. Soc.* **1982**, *104*, 6791–6793.

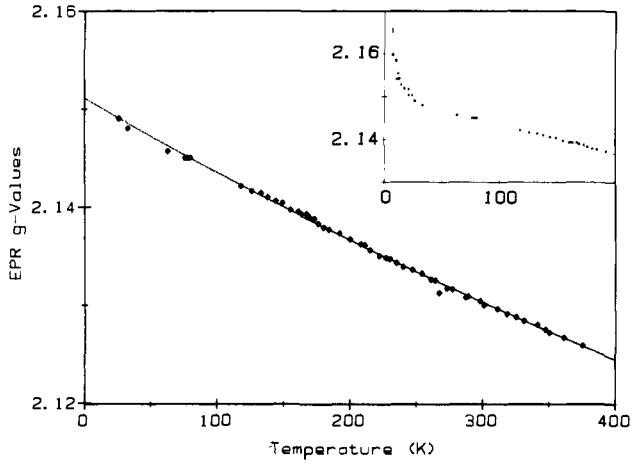

Figure 5. Parallel component ($\phi = 0°$) of the EPR g tensor for a single crystal of Cu(pc)I as a function of temperature. The dotted line represents the best fit to eq 12 as discussed in the text. Inset: low-temperature behavior of g parallel showing a strong increase below 8 K.

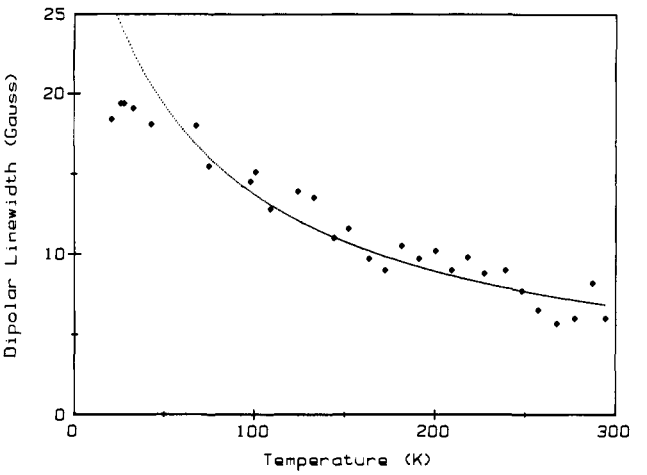

Figure 6. Plot of dipolar line width Γ_1 (eq 13) vs. T. The dotted line represents the best fit of the data to eq 16 as discussed in the text.

would display two distinct resonances. The signal of the localized Cu^{2+} sites would have temperature independent g values similar to those found for Cu(pc)[30] in a diamagnetic Zn(pc) host ($g_\parallel \approx 2.179$, $g_\perp \approx 2.05$); that associated with the oxidized macrocycles would exhibit a temperature independent and roughly isotropic g tensor ($g_\pi \approx 2.00$), as with Ni(pc)I.[4b] Instead, strong exchange coupling ($J >> (g_{Cu} - g_\pi)\mu_B H_0$) between the local and carrier spins causes the EPR spectrum of a single crystal of Cu(pc)I to show a single resonance. At all temperatures, the g tensor is axially symmetric with the unique tensor axis corresponding to the fourfold needle c axis. For a typical crystal of Cu(pc)I at ambient temperatures $g_\parallel = 2.131$ and $g_\perp = 2.031$, values that are intermediate between those expected for isolated Cu(pc) or π-carrier spins. The g values increase when the sample is cooled and approach those of pure Cu(pc) at low temperatures (Figure 5). The g tensor of a system in which two different magnetizations are strongly exchange coupled occurs at the susceptibility weighted average of the individual component g values.[28,31] In the present case, g_{Cu} is the angle-dependent g value of the one-dimensional array of Cu^{2+} spins

$$g_{obsd}(\phi,T) = f(T)g_{Cu}(\phi) + (1 - f(T))g_\pi$$
$$f(T) = \chi_{Cu}{}^{(T)}/(\chi_{Cu}{}^{(T)} + \chi_\pi) \qquad (12)$$
$$g_{Cu}{}^2(\phi) = (g_\parallel{}^{Cu})^2 \cos^2\phi + (g_\perp{}^{Cu})^2 \sin^2\phi$$

g_π is the isotropic g value of the π-carriers, and the angle ϕ is taken between the c axis and the magnetic field.

By using the susceptibility results to calculate $f(T)$, we analyzed the parallel ($\phi = 0$) component of the Cu(pc)I g tensor for $T >$ 20 K (Figure 5) to obtain $g_\parallel{}^{Cu} = 2.151$ and $g_\pi = 1.97$, values similar to, but reduced from, those of the related compounds Cu(pc)[30] and Ni(pc)I.[4b] As shown in the inset to Figure 5, in the range 8 K $< T <$ 20 K, the g value increases above that predicted by eq 12, an effect that is not understood. A similar analysis of the perpendicular component of the EPR g tensor for Cu(pc)I may be made for temperatures above ca. 90 K[32] to give $g_\perp{}^{Cu} = 2.039$.

EPR Line Width Measurements. The orientation dependence of the EPR line widths of Cu(pc)I can be described by the expression

$$\Gamma(\phi) = \Gamma_0 + \Gamma_1(1 + \cos^2\phi) \qquad (13)$$

This is the form expected for a one-dimensional spin system where spin–dipolar interactions are subjected to strong exchange narrowing: exchange frequency (ω_e) > Larmor frequency (ω_0).[33] A nonlinear least-squares fit of the EPR line width data at 293 K to eq 13 yields values of $\Gamma_0 = 12.5$ (3) and $\Gamma_1 = 6.0$ (2) G. The parallel component ($\phi = 0°$) of the line width broadens strongly with decreasing temperature while the perpendicular component ($\phi = 90°$) remains relatively constant down to at least 20 K. In contrast, molecular crystals whose metallic conductivity is dominated by spin–phonon interactions exhibit an EPR line width that decreases upon cooling because of stronger motional narrowing.[34] The temperature response of Γ_{obsd} is best considered in terms of the behavior of Γ_1 and Γ_0 with temperature. Figure 6 presents $\Gamma_1(T)$; the isotropic term, $\Gamma_0(T)$, decreases approximately linearly from $\Gamma_0 = 12.5$ at ambient to $\Gamma_0 \sim 0$ as $T \to 0$.

Extending our treatment of the magnetic properties of Cu(pc)I as arising from two strongly exchange-coupled magnetic subsystems, we decompose the observed EPR line width into the susceptibility weighted sum of the line widths of the local and carrier spin systems

$$\Gamma_{obsd}(T) = f_{Cu}(T)\Gamma^{Cu} + f_\pi(T)\Gamma^\pi \qquad (14)$$

The line width of carrier spins is expected to be nearly isotropic. In contrast, numerous studies[33] of one-dimensional chains of Cu^{2+} complexes show that the interplay of dipolar and exchange coupling between Cu^{2+} sites gives a narrowed, anisotropic EPR signal whose line width (Γ^{Cu}) obeys eq 13. Thus, we assign the anisotropic component (Γ_1) of the Cu(pc)I line width to the Cu^{2+} spin system, in which case $\Gamma_1(T)$ is described by a single-term version of eq 14

$$\Gamma_1(T) = f_{Cu}(T)\Gamma_1{}^{Cu}(T) \qquad (15)$$

For the one-dimensional Heisenberg chain, the contribution of hyperfine interactions is negligibly small, and the anisotropic component is $\Gamma_1{}^{Cu} \approx \Delta\omega_d{}^2/\omega_e$, where $\Delta\omega_d{}^2$ is the dipolar second moment of the chain, and $\omega_e = J$, the exchange interaction between adjacent Cu^{2+} spins. The isotropic component to the line width (Γ_0) is not unambiguously assignable. However, its small value and positive temperature coefficient are reminiscent of the behavior of the line widths associated with the mobile charge carriers of other porphyrinic molecular metals.[4b]

Further analysis of the line width behavior of Cu(pc)I requires a description of the processes that narrow the dipolar line width of the copper spins. The dipolar interactions between local moments would be modulated by quantum mechanical (temperature-independent) exchange between copper centers (frequency, $\omega_e{}^{QM}$).[33,35] This term could include near-neighbor interactions

(30) Harrison, S. E.; Assour, J. M. *J. Chem. Phys.* **1964**, *40*, 365–370.
(31) (a) Alcacer, L.; Maki, A. H. *J. Phys. Chem.* **1976**, *80*, 1912–1916. (b) Tomkiewicz, Y.; Taranko, A. R.; Torrance, J. B. *Phys. Rev. B* **1977**, *15*, 1017–1023. (c) Conwell, E. *Phys. Rev. B* **1980**, *22*, 3107–3112.
(32) At temperatures below 90 K, $g_\perp$ begins to decrease with decreasing temperature. No explanation exists for this second-order effect.
(33) (a) Soos, Z. G.; Huang, T. Z.; Valentine, J. S.; Hughes, R. C. *Phys. Rev. B.* **1973**, *8*, 993–1007. (b) McGregor, K. T.; Soos, Z. G. *J. Chem. Phys.* **1976**, *64*, 2506–2517.
(34) Tomkiewicz, Y.; Taranko, A. R. *Phys. Rev. B* **1978**, *18*, 733–741.
(35) Anderson, P. W.; Weiss, P. C. *Rev. Mod. Phys.* **1953**, *25*, 269–276.

caused by direct Cu–Cu overlap as well as indirect interactions mediated through the itinerant carriers. Studies of isolated local moments exchange-coupled to itinerant spins[28] indicate that one must also allow for a second, temperature-dependent term arising from the dynamic exchange between local and itinerant moments (frequency, $\omega_e^{dyn} \approx T$). We therefore attempt to describe the modulation of the Cu^{2+} spins by an effective frequency of the functional form

$$\omega_e \approx \mathbf{a} + \mathbf{bT}$$

Here **a** represents the sum of direct and indirect quantum mechanical exchange couplings between copper centers and thus should correspond to θ; **bT** represents the dynamical exchange between local and mobile spins. If this form is inserted into the standard expression for the dipolar line width in the strong exchange limit, eq 15 becomes

$$\Gamma_1 \sim f_{Cu}(T)\left(\frac{\Delta\omega_d^2}{\omega_e}\right) = f_{Cu}(T)\left(\frac{\Delta\omega_d^2}{\mathbf{a} + \mathbf{bT}}\right) \qquad (16)$$

The values $\hbar\omega_e^{QM}/k_B = \hbar a/k_B = 3.6$ K and $\hbar b/k_B = 3.1 \times 10^{-2}$ are obtained from a nonlinear least-squares analysis of the line width data, with the use of $f_{Cu}(T)$ as obtained from the static susceptibility measurements and $\Delta\omega_d^2 = 3.3 \times 10^{18}$ Hz^2, as calculated from standard expressions.[33] As seen in Figure 6, the resulting equation fits the data reasonably well. At 300 K, $\hbar\omega_e/k_B \approx 13$ K, and dynamic exchange accounts for approximately 72% of the total, whereas at 20 K, $\hbar\omega_e/k_B \approx 4.3$ K, and static interactions contribute 84% of the total effective exchange interaction. The correspondence of exchange energies from two very different methodologies, namely the equality of θ from static susceptibility measurements and $\hbar\omega_e^{QM}/k_B$ from EPR line width data, lends support to the heuristic description presented here for the strong exchange coupling between the local and carrier spins.

Summary

The chemical flexibility of the metallophthalocyanine building blocks has allowed us to incorporate a one-dimensional array of paramagnetic local moments into the conducting framework of an organic conductor. Cu(pc)I is a highly conductive molecular crystal ($\sigma_{RT} \approx 10^3\ \Omega^{-1}\ cm^{-1}$) that remains metallic at least down to 10 K. The charge carriers of this material are associated with the organic pc ligand, and the Cu^{2+} sites embedded within each conducting stack form a one-dimensional chain of $S = {}^1/_2$ paramagnets. Recently,[36-40] other systems have been prepared in which localized moments are placed in close proximity to itinerant π-carriers by cocrystallizing inorganic complexes with various organic conductors. However, no other material displays local moments and charge carriers within a *single* conductive stack or the high conductivity found in Cu(pc)I.

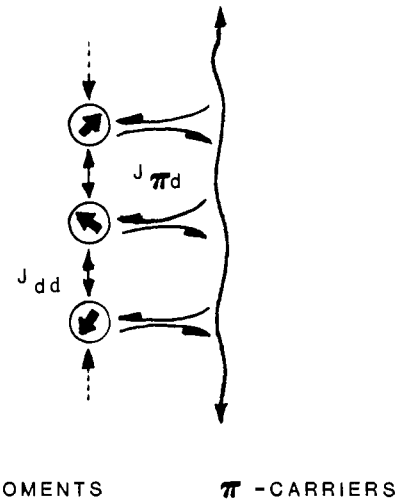

Figure 7. Schematic representation of Cu(pc)I, where a dense, one-dimensional array of Cu^{2+} spins may interact among themselves (represented by J_{dd}) or couple to the itinerant π-electron carriers of the pc ring. The latter coupling (represented by $J_{\pi d}$) may have quantum mechanical and dynamic contributions (see text).

Susceptibility and EPR studies demonstrate that the one-dimensional local and mobile spin systems of Cu(pc)I are exchange-coupled by dynamic and quantum mechanical terms. In addition, Cu^{2+} sites exhibit dipolar interactions that are modulated by these terms. This novel system is sketched in Figure 7. The analogous case of isolated magnetic impurities in three-dimensional atomic metals, which produces anomalous physical properties such as the Kondo transition at low temperatures,[8] remains a challenge to theorists. The situation in Cu(pc)I is analogous but differs in some important ways: Cu(pc)I presents local moments coupled to carrier spins in a one-dimensional array, and the local moments in this magnetically concentrated material interact strongly among themselves. An intriguing consequence of this situation is the observation of a new type of low-temperature phase transition in Cu(pc)I that involves the coupled local and itinerant spin systems of this unique molecular metal.[6b,c]

Acknowledgment. This work was supported by the National Science Foundation through the Solid State Chemistry program, Grant No. DMR 8519233 (B.M.H.), and the NSF-MRL program, Grant No. DMR 8520280, to the Northwestern University Materials Research Center.

Registry No. Cu(pc), 147-14-8.

Supplementary Material Available: Table III, anisotropic thermal parameters (1 page); Table IV, structure factor amplitudes (5 pages). Ordering information is given on any current masthead page.

(36) (a) Alcacer, L.; Novais, H.; Pedroso, F.; Flandrois, S.; Coulon, C.; Chasseau, D.; Gaultier, J. *Solid State Commun.* **1980**, *35*, 945–949. (b) Henriques, R. T.; Alcacer, L.; Pouget, J. P.; Jerome, D. *J. Phys. C* **1984**, *17*, 5197–5208.

(37) Lacrojx, P.; Kahn, O.; Gleizes, A.; Valde, L.; Cassoux, P. *Nouv. J. Chem.* **1984**, *8*, 643–651.

(38) Batail, P.; Ouahab, L.; Torrance, J. B.; Pylman, M. L.; Parkin, S. S. P. *Solid State Commun.* **1985**, *55*, 597–600.

(39) Heuer, W. B.; Hoffman, B. M. *J. Chem. Soc., Chem. Commun.* **1986**, 174–175.

(40) Inoue, M.; Inoue, M. B. *Inorg. Chem.* **1986**, 25, 37–41.